Supplementary materials

Future changes of global potential evapotranspiration simulated from CMIP5 to CMIP6 models

LIU Xinlei[a] , LI Chunxiang[b], ZHAO Tianbao[b] and HAN Lin[a]

[a]School of Atmospheric Sciences, Chengdu University of Information Technology, Chengdu, China; [b]Key Laboratory of Regional Climate-Environment Research for East Asia, Institute of Atmospheric Physics, Chinese Academy of Sciences, Beijing, China

Table S1. CMIP5 modes used in this study.

Model	Resolution (lon×lat)	Research institute and country
ACCESS1-3	1.875°×1.241°	Commonwealth Scientific Industrial Research Organization and Bureau of Meteorology, Australia
CanESM2	2.813°×2.813°	Canadian Centre for Climate Modelling and Analysis, Canada
CNRM-CM5	1.406°×1.406°	Centre National de Recherches Météorologiques/Centre Européen de Recherche et Formation Avancées en Calcul Scientifique, France
CSIRO-Mk3-6-0	1.875°×1.875°	Queensland Climate Change Centre of Excellence and Commonwealth Scientific and Industrial Research Organization, Australia
GFDL-CM3	2.500°×2.000°	Geophysical Fluid Dynamics Laboratory, USA
GFDL-ESM2G	2.500°×2.000°	Geophysical Fluid Dynamics Laboratory, USA
GISS-E2-H	2.500°×2.000°	NASA Goddard Institute for Space Studies, USA
GISS-E2-R	2.500°×2.000°	NASA Goddard Institute for Space Studies, USA
HadGEM2-CC	1.875°×1.241°	Meteorological Office Hadley Centre, UK
HadGEM2-ES	1.875°×1.241°	Meteorological Office Hadley Centre, UK
inmcm4	1.875°×1.241°	Institute for Numerical Mathematics, Russia
IPSL-CM5A-LR	3.750°×1.895°	Institute Pierre-Simon Laplace, France
MIROC5	1.406°×1.406°	University of Tokyo, National Institute for Environmental Studies/Japan Agency for Marine-Earth Science and Technology, Japan
MIROC-ESM	2.813°×2.813°	University of Tokyo, National Institute for Environmental Studies/Japan Agency for Marine-Earth Science and Technology, Japan
MIROC-ESM-CHEM	2.813°×2.813°	University of Tokyo, National Institute for Environmental Studies/Japan Agency for Marine-Earth Science and Technology, Japan
MRI-CGCM3	1.125°×1.125°	Meteorological Research Institute, Japan

Table S2. CMIP6 modes used in this study.

Model	Resolution (lon×lat).	Research institute and country
CanESM5	2.813°×2.813°	Canadian Centre for Climate Modelling and Analysis, Canada
CESM2	1.250°×0.938°	National Center for Atmospheric Research, Climate and Global Dynamics Laboratory, USA
CESM2-WACCM	1.250°×0.938°	National Center for Atmospheric Research, Climate and Global Dynamics Laboratory, USA
EC-Earth3-Veg	2.500°×2.000°	NASA Goddard Institute for Space Studies, USA
IPSL-CM6A-LR	2.500°×1.259°	Institute Pierre-Simon Laplace, France
MIROC6	1.406°×1.406°	University of Tokyo, National Institute for Environmental Studies/Japan Agency for Marine-Earth Science and Technology, Japan
MRI-ESM2-0	1.125°×1.125°	Meteorological Research Institute, Japan

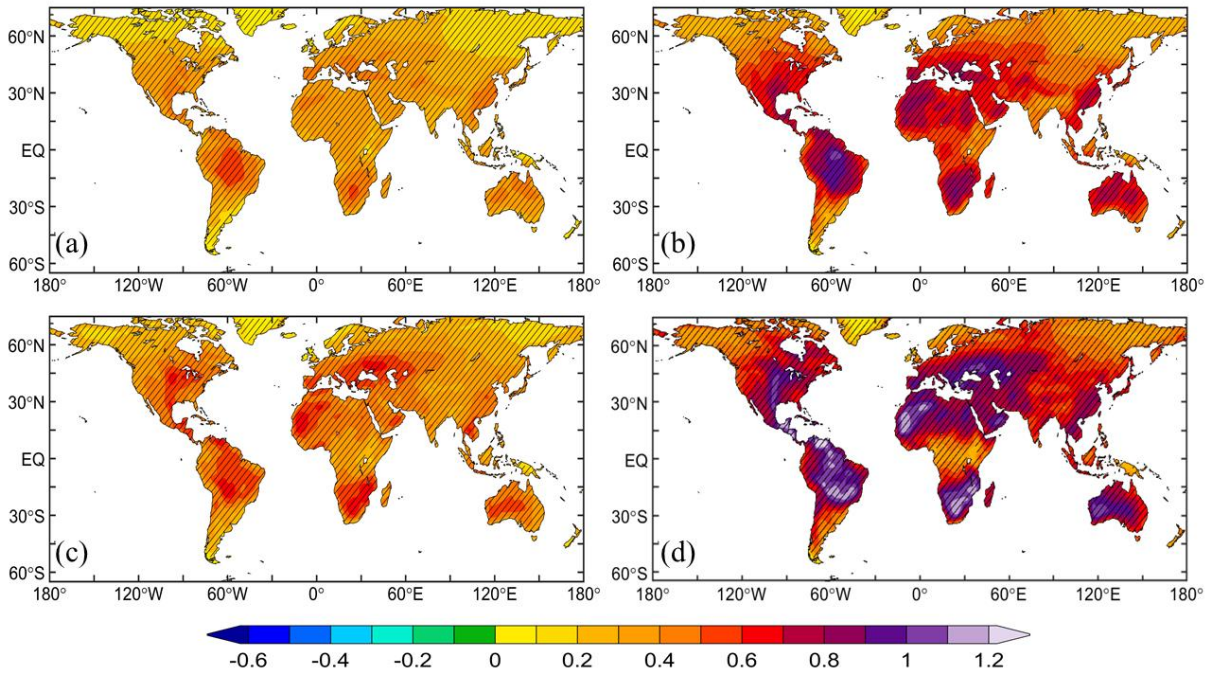

Figure.S1 Spatial distribution of long-term changes in the annual PET (units: mm day^{-1}) from 1979–99 to 2079–99 over land areas. **(a)** CMIP5 ensemble mean under the RCP4.5 scenario, **(b)** CMIP5 under the RCP8.5 scenario, **(c)** CMIP6 under the SSP2.45 scenario and **(d)** CMIP6 under the SSP5.85 scenario. The shading indicates that at least 80% of the models agree on the sign of the change.

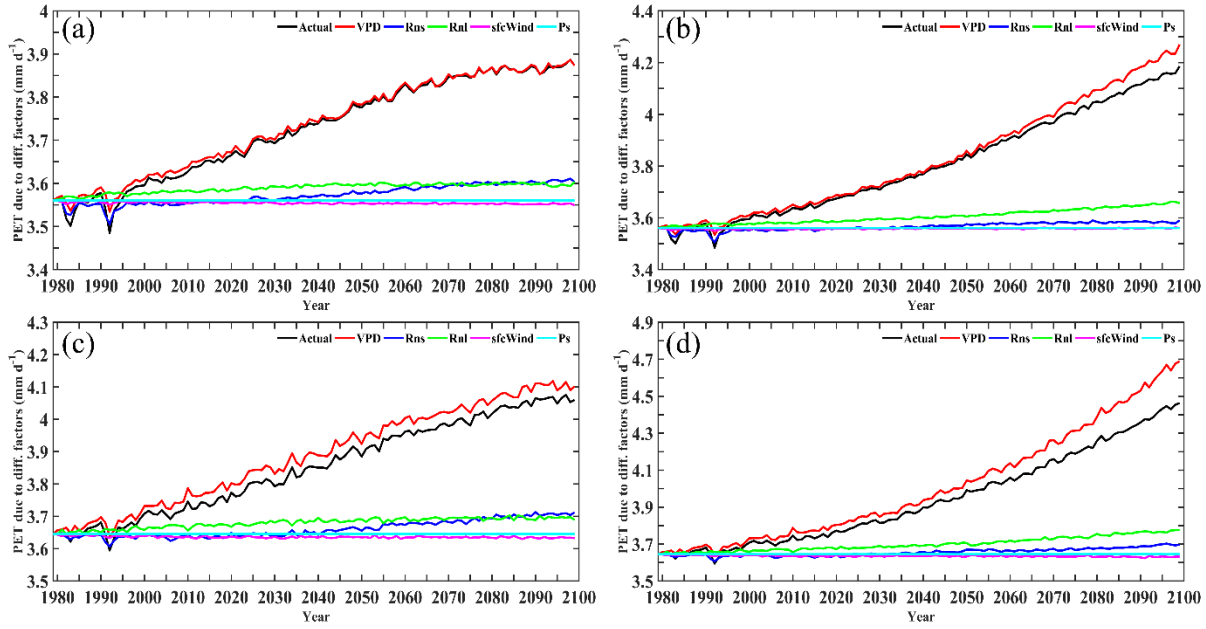

Figure.S2 Time series of interannual changes in the contribution of the multi-model ensemble mean driving factors for each PET over global land areas (60°S–75°N) (units: mm day^{-1}). **(a)** CMIP5 under the RCP4.5 scenario, **(b)** CMIP5 under the RCP8.5 scenario, **(c)** CMIP6 under the SSP2.45 scenario and **(d)** CMIP6 under the SSP5.85 scenario. Changes corresponding to the actual changes in PET (black) and PET caused by the vapor pressure deficit (*VPD*, red), shortwave radiation (*Rns*, blue), longwave radiation (*Rnl*, magenta), surface wind speed (*sfcWind*, green) and surface pressure (*Ps*, turquoise).